Mutations in TOP3A Cause a Bloom Syndrome-like Disorder

Mutations in *TOP3A* cause a Bloom's syndrome-like disorder

Carol-Anne Martin[1*], Kata Sarlós[2*], Clare Logan[1*], Roshan Singh Thakur[2*], David Parry[1], Anna H. Bizard[2], Andrea Leitch[1], Louise Cleal[1], Nadia Shaukat Ali[3], Mohammed A. Al-Owain[4], William Allen[5], Janine Altmüller[6], Miriam Aza-Carmona[7,8,], Bushra A Y Barakat[3], Jimena Barraza-García[7,8,], Amber Begtrup[9], Massimo Bogliolo[8,10], Megan T. Cho[9], Jaime Cruz-Rojo[11], Hassan Ali Mundi Dhahrabi[3], Nursel H. Elcioglu[12], GOSgene[13], Gráinne S. Gorman[14], Rebekah Jobling[15], Ian Kesterton[16], Yoshihito Kishita[17], Masakazu Kohda[17], Polona Le Quesne Stabej[13], Asam Jassim Malallah[3], Peter Nürnberg[6], Akira Ohtake[18], Yasushi Okazaki[17], Roser Pujol[8,10], Maria José Ramirez[8,10], Anya Revah-Politi[19], Masaru Shimura[20], Paul Stevens[16], Robert W. Taylor[14], Lesley Turner[21], Hywel Williams[13], Carolyn Wilson[5], Gökhan Yigit[22], Laura Zahavich[15], Fowzan S. Alkuraya[23,$], Jordi Surralles[8,10,24,$], Alejandro Iglesais[25,$], Kei Murayama[20,$], Bernd Wollnik[22,$], Mehul Dattani[13,$], Karen E. Heath[7,8,$], Ian D. Hickson[2,&], Andrew P Jackson[1,&]

*equal contributing first authors
[$]equal contributing senior authors
[&]corresponding authors

Correspondence to Andrew.Jackson@igmm.ed.ac.uk
iandh@sund.ku.dk

[1] MRC Human Genetics Unit, MRC Institute of Genetics and Molecular Medicine, University of Edinburgh, Edinburgh EH4 2XU, UK.

[2] Center for Chromosome Stability and Center for Healthy Aging, Department of Cellular and Molecular Medicine, University of Copenhagen, Blegdamsvej 3B, 2200 Copenhagen N, Denmark

[3]Dubai Hospital, Albaraha Street, PO Box 7272, Postal code 0000, Dubai

[4]Department of Medical Genetics, King Faisal Specialist Hospital and Research Center, Riyadh 11211, Saudi Arabia

[5]Fullerton Genetics Center, Asheville, North Carolina, NC 28803

[6]Cologne Center for Genomics, University of Cologne, 50931 Cologne, Germany

[7]Institute of Medical and Molecular Genetics (INGEMM) and Skeletal dysplasia multidisciplinary Unit (UMDE), Hospital Universitario La Paz, UAM, IdiPaz, Madrid, 28046, Spain

[8]Centro de Investigación Biomédica en Red de Enfermedades Raras (CIBERER), Madrid, 28029, Spain

[9]GeneDx, 207 Perry Parkway, Gaithersburg, MD 20877, USA

[10]Department of Genetics and Microbiology, Universitat Autònoma de Barcelona, Bellaterra, 08193, Spain

[11]Dept of Pediatric Endocrinology & Dysmorphology, Hospital 12 Octubre, Madrid, 28041, Spain

[12]Department of Pediatric Genetics, Marmara University Medical School, Istanbul, 34722, Turkey

[13]UCL Great Ormond Street Institute of Child Health, 30 Guilford Street, London WC1N 1EH, UK

[14]Wellcome Centre for Mitochondrial Research, Institute of Neuroscience, The Medical School, Newcastle University, Newcastle upon Tyne, NE2 4HH, UK

[15]The Hospital for Sick Children, Toronto, M5G 1X8, Canada

[16]Cytogenetics Department, Viapath Analytics, Guy's Hospital, London, SE1 9RT, UK

[17] Intractable Disease Research Center, Graduate School of Medicine, Juntendo University, 2-1-1, Hongo, Bunkyo-ku, Tokyo, 113-8421, Japan

[18] Department of Pediatrics, Faculty of Medicine, Saitama Medical University, 38 Morohongo, Moroyama, Saitama 350-0495, Japan

[19] Institute for Genomic Medicine, Columbia University Medical Center, New York, NY 10032, USA

[20] Center for Medical Genetics, Department of Metabolism, Chiba Children's Hospital, 579-1 Heta-cho, Midori-ku, Chiba, 266-0007, Japan

[21] Memorial University of Newfoundland, St. John's, Newfoundland, A1C 5S7, Canada

[22] Institute of Human Genetics, University Medical Center Göttingen, 37073 Göttingen, Germany

[23] Department of Genetics, King Faisal Specialist Hospital and Research Center, Riyadh 11211, Saudi Arabia

[24] Department of Genetics and Biomedical Research Institute Sant Pau (IIB Sant Pau), Hospital de la Santa Creu i Sant Pau, Barcelona, 08041, Spain

[25] Department of Pediatrics, Division of Clinical Genetics, Columbia University Medical Center, New York, NY 10032, USA

Abstract (250words)

Bloom's syndrome, caused by biallelic mutations in *BLM*, is characterised by prenatal onset growth deficiency, short stature, an erythematous photosensitive malar rash and increased cancer predisposition. Diagnostically, a hallmark feature is the presence of increased sister chromatid exchanges (SCEs) on cytogenetic testing. Here, we describe biallelic mutations in *TOP3A* in ten individuals with prenatal-onset growth restriction and microcephaly. *TOP3A* encodes topoisomerase III alpha (TopIIIα), which binds to BLM as part of the BTRR protein complex, and promotes dissolution of double Holliday junctions arising during homologous recombination. We also identify a homozygous truncating variant in *RMI1,* that encodes another component of the BTRR complex, in two individuals with microcephalic dwarfism. The *TOP3A* mutations substantially reduce cellular levels of TopIIIα protein and consequently subjects' cells demonstrate elevated rates of SCE. Unresolved DNA recombination and/or replication intermediates persist into mitosis leading to chromosome segregation defects and genome instability that likely explain the growth restriction seen in these subjects and in Bloom's syndrome. Clinical features of mitochondrial dysfunction are evident in several individuals with biallelic *TOP3A* mutations, consistent with the recently reported additional function of TopIIIα in mitochondrial DNA decatenation. In summary, our findings establish *TOP3A* mutations as an additional cause of prenatal-onset short stature with increased cytogenetic SCEs, and implicate the decatenation activity of the BTRR complex in their pathogenesis.

Introduction

Microcephalic primordial dwarfism (MPD) is used to collectively describe a heterogeneous group of disorders characterized by significant *in utero* and postnatal growth retardation alongside marked microcephaly[1]. Bloom's syndrome (MIM 210900) is also associated with prenatal growth restriction, short stature and microcephaly. It is distinguished by an erythematous sun-sensitive facial rash that may become evident during childhood[2]. A predisposition to the development of cancer in early adulthood is also seen, with both solid tumours and haematological malignancies a major cause of early death[3]. Additionally, a key cytogenetic feature of Bloom's syndrome is an increased number of sister chromatid exchanges (SCEs)[4]. Notably, when molecular testing is inconclusive, a finding of elevated SCEs is currently utilised for diagnostic confirmation of Bloom's syndrome.[5]

In 1995, Bloom's syndrome was shown to be caused by mutations in *BLM,* which encodes a RecQ family DNA helicase[6]. Mutations in *BLM* are typically biallelic loss-of-function mutations[7]. BLM forms the BTRR protein complex with Topoisomerase III alpha (TopIIIα), and the RecQ-mediated genome instability proteins 1 and 2 (RMI1 and RMI2). Together, these proteins process double Holliday junctions (dHJ) that arise due to homologous recombination-mediated repair of dsDNA breaks during DNA synthesis[8-14]. The process of dHJ dissolution requires two steps. Firstly, the BTRR complex promotes the convergent branch migration of the dHJ to create a hemicatenane intermediate, and then this structure is decatenated by TopIIIα in concert with RMI1/2[15; 16]. Dissolution of a dHJ by this mechanism can be completed without any potentially detrimental exchanges between genetic markers flanking the original site of homologous recombination. The alternative

processing of dHJ by the HJ resolvases (SLX-MUS81 and GEN1 nucleases) can yield cross over events, and it is increased usage of this pathway that has been proposed to explain the increase in SCEs in BLM-deficient cells [17]. Cross-over events between homologous chromosomes can lead to loss of heterozygosity (LOH)[18], which can be detrimental to cell survival and contribute to increased cancer predisposition[19]. Additionally, unresolved recombination intermediates can persist into mitosis leading to chromosome bridges and act as a source of genome instability[20].

Here, we report the identification of pathogenic mutations in *TOP3A* in ten individuals with Bloom's syndrome-like phenotypic features, and characterise the cellular consequences of these mutations.

Material and Methods

Research subjects

Genomic DNA from the affected individuals and family members was extracted from peripheral blood by standard methods or obtained from saliva samples using Oragene collection kits according to the manufacturer's instructions. Informed consent was obtained from all participating families and all procedures performed in studies involving human participants were in accordance with the Declaration of Helsinki. Research studies were approved by the Scottish Multicentre Research Ethics Committee (05/MRE00/74); the Hospital Universitario La Paz ethical committee (PI-2630); the GOSH Research Ethics Committee (09/H0706/66); the University Medical Center Göttingen Ethics Committee (Vote Ref 3/2/1) and the Institute for Genomic Medicine at Columbia University (protocol AAAO8410).

Parents provided written consent for the publication of photographs of the affected individuals. For growth measurements, Z-scores (standard deviations from population mean for age and sex) were calculated using LMS growth based on British 1990 growth reference data [21]. For calculation of Z-scores for growth measurements published for Bloom's syndrome [22], full-term gestation was assumed, and post-natal growth measurements calculated from data provided for the 18-21 year age range.

Exome sequencing and Sanger sequencing

Exome sequencing and confirmatory capillary Sanger sequencing were performed using standard methodologies as previously published[23; 24]. TOP3A and RMI1 variants were annotated using NM_004618.4 and NM_024945.2 reference sequences respectively.

Plasmid Construct and protein purification

Cloning of the mutant hTopIIIα expression vector: A plasmid encoding the wild type *TOP3A* cDNA[25] was modified by Quickchange XL Site directed mutagenesis kit (Agilent technologies) with the following primers to recapitulate the deletion and frame-shift present in subject P1: T3_FS_FW: 5'- CCCTCCGTCACACGACTGTGCAGAAGGA -3' and T3_FS_RW: 5'-TCCTTCTGCACAGTCGTGTGACGGAGGG -3'.

Expression and purification of TRR: The previously described plasmids encoding RMI1 and RMI2[14] and hTopoIIIα[25] were co-transformed into *E. coli* Rosetta 2 cells, and the complex was expressed. The cells were disrupted in buffer A (50 mM Tris-HCl, pH 7.5, 0.5 M NaCl, 10% glycerol, 0.1 % Igepal, 2 mM β-mercaptoethanol, 40 mM Imidazole, 1 mM PMSF, protease inhibitor tablet (PI, EDTA-free, Roche)) on ice, before dounce homogenization and sonication. After removal of cell debris by centrifugation, the lysate was affinity-purified on a 5 ml HisTrap

HP affinity column. The complex was further purified on a 5 ml HiTrap Heparin HP column in buffer B (50 mM Tris-HCl, pH 7.5, 10% glycerol, 0.1 mM EDTA, 1 mM DTT) with a linear gradient of 200 mM - 1 M NaCl, followed by gel filtration on a 120 ml HiLoad 16/600 Superdex 200 column in buffer B containing 200 mM NaCl. Expression and purification of the mutant $T^{Thr812LeufsTer101}RR$ complex was performed in a similar manner. BLM was purified as described previously[26 27].

Double-Holliday Junction dissolution: The dHJ substrate construction and dissolution reactions were carried out as described previously[15].

Cell culture

Dermal fibroblasts were obtained by skin punch biopsy and were maintained in amnioMAX C-100 complete medium (Life Technologies) in a 37°C incubator with 5% CO_2 and 3% O_2. siRNA oligonucleotides (siLUC: CUUACGCUGAGUACUUCGA, siTopIIIα SMARTpool M-005279-01-0005(Dharmacon)) were transfected into dermal fibroblasts cells using RNAiMAX (Life Technologies) according to the manufacturer's instructions.

Sister Chromatid Exchange Assay

Dermal fibroblasts were treated with 10 µM BrdU for 48 hrs followed by 0.5 µg/ml Colcemid for 2 hrs. Metaphases and nuclei were isolated in hypotonic buffer (0.25% KCl, 1% $Na_3C_6H_5O_7$), fixed with methanol:acetic acid (3:1), and dropped onto slides. Dried slides

were rehydrated in PBS and then incubated with 2 μg/ml Hoescht 33342 stain in 2x SSC buffer (300mM NaCl, 30mM sodium citrate) for 15 mins. Slides were then covered in 2x SSC buffer and irradiated in UV-A at 5400 J/m^2. Dehydrated in an ethanol series and mounted in vectashield with DAPI.

SCE Methodology for analysis P7,P8 : Dermal fibroblasts were treated with 26.05 μM of BrdU for 72 hrs followed by 0.5 μg/mL Colcemid for 5 hrs and then harvested. Cells resuspended in a pre-warmed hypotonic solution (0.051 M KCl) for 20 min at 37 ºC, then fixed with acetic acid: methanol (1:3 vol/vol) and dropped onto slides. Samples were aged for at least 3 days, then stained with 1.56 μg/ml Hoechst 33258 (Sigma, B2883). Slides irradiated in 2xSSC with UVC (356 nm) 0.260 J/cm2, washed with 2xSSC, and stained with 10% Giemsa in phosphate buffer.

SCE analysis of peripheral blood samples was performed using standard methodology in a diagnostic lab setting[28].

Immunofluorescence and microscopy

Mitotic abnormalities and G1-associated defects were analyzed as described previously[29; 30]. Briefly, for mitotic analysis, cells were seeded onto 22 x 22 mm glass coverslips in 6 well plates. After 18 hrs, cells were treated with 3.5 μM RO3306 for 6 hrs to induce a late G2 arrest, and were subsequently released into fresh media. After 45 mins, cells were fixed with 4% paraformaldehyde containing 0.2% Triton X-100 in PBS for 20 mins. For G1-associated defects, RO3306 treated cells were released into fresh media for 30 mins. Prometaphase cells were shaken off and re-seeded onto poly-L-lysine coated glass slides. After 4-6 hrs, cells were fixed with 4% paraformaldehyde for 10 mins and permeabilized with 0.5% Triton X-100 for 10 mins. Fixed cells were incubated with antibodies specific for

Cyclin A (Santa Cruz Biotechnology, sc-596), 53BP1 (Santa Cruz Biotechnology, sc-515841) and PICH[31].

Western blotting

Cells were lysed in 50 mM Tris-HCl (pH 8), 280 mM NaCl, 0.5% NP40, 0.2 mM EDTA, 0.2 mM EGTA, and 10 % glycerol supplemented with protease inhibitor tablet (Roche Life Science). Protein samples were run on a 4–12 % NuPAGE Bis-Tris precast gel (Life Technologies) followed by immunoblotting using anti-TopIIIα raised against amino acids 652-1001 (Proteintech, 14525-1-AP) and actin (Sigma, A2066).

Results

Identification of mutations in *TOP3A*

In ongoing work to identify novel microcephalic dwarfism genes, whole exome sequencing (WES) was performed on subject P1, who had significant microcephaly and short stature (-4.7 and -4.4 standard deviations (s.d.) respectively). This identified a homozygous frameshift mutation NM_004618.4: c.2718del (p.Thr907LeufsTer101) in *TOP3A* located on chromosome 17p11.2. Following interrogation of other cohorts and through clinical contacts made through GeneMatcher[32], we subsequently ascertained a further nine individuals from seven families with biallelic deleterious *TOP3A* variants that had also been discovered by WES (Table 1). All variants identified were validated by Sanger capillary sequencing, and all parents were confirmed to be heterozygous carriers. Aside from the c.2718del variant (MAF 0.00041%), none of the other variants were reported in GnomAD[33].

Notably, four of the families from UAE, Syria and Saudi Arabia (F2, F4, F6 and F7), were homozygous for the same variant.

Prenatal-onset growth restriction and microcephaly in *TOP3A* Individuals

Prenatal growth restriction was evident, with substantially reduced birth weight in all individuals (mean weight -2.6 ± 0.9 standard deviations, s.d.) (Table 2, Figure 1A). Postnatally, both weight (mean weight -4.8 ± 1.8 s.d.), height (mean height -3.9 ±1.0 s.d.) and head circumference (mean OFC -4.0 ±1.2 s.d.) were significantly reduced. Growth parameters were similar to those previously reported for Bloom's syndrome (mean birth weight -3.7 ± 1.2 s.d.; mean postnatal weight -3.8 ± 2.1 s.d.; mean height -3.9 ± 1.1 s.d.) [22]. While multiple café-au-lait patches were present in some *TOP3A* individuals, the classical erythematous malar facial rash was not apparent and nor were there any reports of malignancies (although none had yet reached adulthood, Table 3, Figure 1B).

Cardiomyopathy is present in some *TOP3A* subjects

A single individual compound heterozygous for rare *TOP3A* variants has been reported recently with an adult-onset mitochondrial disorder (denoted as MC1 in Table 1) [34]. While stature was normal in this individual (adult female, 163 cm), several of the subjects reported here had clinical features that could also be attributable to mitochondrial dysfunction. P3, P4 (family 2) had an additional diagnosis of dilated cardiomyopathy, which proved fatal in P4 at age 10. Another brother in this sibship died aged 13 of cardiomyopathy. Morphometric and other clinical information are not available for this case. In P5 (family 3), a dilated cardiomyopathy was also reported, with skeletal muscle biopsy demonstrating 87% mitochondrial DNA depletion. P8 also had asymptomatic left ventricular dilatation noted on echocardiography, while P9 had hypertrophic cardiomyopathy.

Given the identification of multiple individuals with biallelic deleterious variants in *TOP3A*, alongside a consistent clinical phenotype across the cohort, we concluded that these mutations were likely to be pathogenic. We therefore pursued confirmatory functional studies, employing both biochemical and cell biological approaches.

***TOP3A* mutations lead to marked reduction in cellular levels of the TopIIIα enzyme**

Most of the identified *TOP3A* mutations are predicted to prematurely truncate the encoded protein (Figure 2A), and hence are likely to have significant effects on cellular protein levels. We therefore assessed the levels of TopIIIα in primary dermal fibroblast cell lines derived from P1, P7 and P8. Immunoblotting demonstrated that the level of full-length TopIIIα protein was substantially reduced in total cell lysates from all three individuals compared to cell lines from unrelated control and parents (Figure 2B).

In most subjects, the frameshift mutations would be expected to result in nonsense-mediated decay of *TOP3A* transcripts, explaining consequent loss of TopIIIα protein. However, the homozygous frameshift mutation in P1 (p.Thr907LeufsTer101) is at the 3' end of the gene, was not predicted to result in NMD and instead would result in a protein of similar length to the wild-type enzyme (TopIIIα^{Thr907LeufsTer101}). The frameshift did, however, result in abolition of the C terminal zinc finger domain whose precise cellular function remains to be defined. We therefore expressed recombinant TopIIIα^{Thr907LeufsTer101} protein in *E.coli*, and purified it to homogeneity as a complex with the co-expressed RMI1 and RMI2 proteins in order to characterise it further. Notably, in contrast to the TRR complex containing TopIIIα^{WT} protein, the complex containing TopIIIα^{Thr907LeufsTer101} protein (hereafter referred to as TopIIIα^{P1}) exhibited reduced stability during purification, with lower yields and increased levels of degradation products evident on SDS-PAGE (Figure 2C). Nevertheless,

when used in equimolar quantities to TopIIIα^{WT}, TopIIIα^{P1} was proficient in a biochemical assay for double Holliday junction (dHJ) dissolution when combined with other components of the BTRR complex. This indicates that this TopIIIα variant retains a near normal level of ssDNA decatenation activity (Figure 2D-F). Therefore, we concluded that the major consequence of the TopIIIα^{Thr907LeufsTer101} mutation, like the other truncating mutations, is severe depletion of TopIIIα enzymatic activity in cells.

P5 was the only individual we identified with an amino acid substitution, p.Ala176Val, which was present *in trans* with a frameshift mutation. The amino acid substitution is absent from GnomAD and *in silico* analyses predict the variant to be deleterious (Mutation Taster, CADD, SIFT). It is at a highly conserved residue (Figure S1) within the TOPA domain (Figure 2A), and would, therefore, be expected to be highly deleterious to enzymatic function.

Given that *Top3a* is a developmentally essential gene in mouse[35], coupled with the above results, we concluded that all the identified mutations result in marked, but most likely hypomorphic, loss of function of TopIIIα due to a reduction in the cellular level of the protein. Therefore, these mutations would be predicted to severely compromise the decatenation activity of the BTRR complex in dHJ dissolution *in vivo*. To assess this possibility, we next pursued cellular assays assessing SCE frequency.

SCEs are markedly elevated in *TOP3A* subjects

dHJ can be processed by two pathways; firstly, dissolution by the BTRR complex yields non-crossover products only; secondly, resolution by endonucleases that cleave HJ structures generate both non-crossovers and crossover products that are visualized as SCEs (Figure 3A). To determine if dHJ dissolution is impaired in the cells of affected individuals, we

assessed the frequency of SCEs. Following BrdU incorporation, we performed differential sister chromatid staining on primary fibroblasts and PHA-stimulated peripheral blood leukocytes (Figure 3B, C). *TOP3A* subject cells had a substantially higher number of SCEs, demonstrating a 3-6 fold increase compared to cells from controls or heterozygous parents (Figure 3C, p-value, $p<0.005$ for all affected individual cell lines). Therefore, excessive crossover recombination was evident in all *TOP3A* subjects tested, indicating that diagnostic cytogenetic assessment of SCE levels is predictive of *TOP3A* mutations as well as *BLM* mutations.

Chromosome segregation defects and genome instability occur in *TOP3A* cells

Impaired decatenation of dHJ may result in persistently entangled sister chromatids that impede chromosome segregation at mitosis[20]. Therefore, we performed detailed characterisation of the mitotic consequences of TopIIIα deficiency in primary fibroblasts from P1. DAPI-staining demonstrated elevated levels of chromatin bridges (Control, C=0, Parent=0.3 ± 0.4, P1=4 ± 0.6) and lagging chromatin/chromosomes (Figure 4A,B) (C=0.9 ± 0.2, Parent=4 ± 0.7, P1=9.2 ± 0.9), consistent with persisting chromosome entanglements. Additionally, increased numbers of ultrafine DNA bridges were seen, revealed by immunostaining for the PICH protein on DAPI-negative regions[20] (C=2.7 ± 0.3, Parent=13.1 ± 1.1, P1=26.7 ± 3.8).

We then examined the post-mitotic consequences of the observed chromosome segregation errors, enriching for G1 cells (Fig. 4C, D). Micronuclei often arise from chromosome segregation errors[36], and analysis of DAPI-stained cells demonstrated substantial numbers of micronucleated cells in the P1 fibroblast cell line compared to control and parental cell lines (Control=0.4 ± 0.2, Parent=1.8 ± 0.5, P1=7.5 ± 1.4). Elevated

levels of 53BP1 nuclear bodies were also seen in cyclin A-negative (G1) cells, indicative of transmission of DNA damage from one cell cycle to the next[37] (Control=0.8 ± 0.3, Parent=4.5 ± 0.5, P1=11 ± 1.7). Taken together, we conclude that impaired dHJ decatenation in TopIIIα deficient cells results both in abnormal recombination and mitotic errors that lead to accumulation of DNA damage. As chromatin bridges and UFBs are also present in Bloom's syndrome individuals[20] these findings are concordant with a shared disease mechanism.

A homozygous truncating variant in *RMI1* associated with microcephalic dwarfism

Finally, through whole exome sequencing we also identified a homozygous truncating variant in *RMI1* (c.1255_1259del, p.Lys419Leufs*5) in two affected cousins (P11, P12) from a consanguineous Turkish family (F8, Table 1, Fig. S3). Both individuals also had microcephalic dwarfism with a similar clinical phenotype and level of growth restriction as *TOP3A* subjects (Fig 1A, Table 2, 3).

Discussion

Here, we report that biallelic mutations in *TOP3A* cause prenatal growth restriction, microcephaly and short stature, a clinical phenotype that overlaps with that seen in Bloom's syndrome. Furthermore, we identify a rare *RMI1* truncating variant (allele frequency, 1.1×10^{-5}) in two individuals. As no homozygous loss of function variants are reported in gnomAD, we expect this to be the cause of microcephalic dwarfism in P11 and P12. However, further case identification with other deleterious sequence variants will be necessary to establish *RMI1* as a disease gene.

Notably, *TOP3A* individuals exhibit elevated SCEs on cytogenetic testing. While cell

362 lines were not available from P11 and P12, we also predict that increased SCE will occur in
363 cells with the homozygous *RMI1* p.Lys419Leufs*5 variant, given the important role of this
364 protein in the BTRR complex[10; 11; 38]. For many years, the diagnosis of Bloom's syndrome
365 rested on a demonstration of elevated SCEs, and this has continued to be employed in cases
366 where molecular testing is inconclusive[5]. Hence, analysis of other BTRR components is now
367 warranted when elevated SCEs are detected. Indeed, given the clear phenotypic overlap
368 between Bloom's syndrome and *TOP3A* individuals, re-evaluation of previous
369 cytogenetically-diagnosed Bloom's syndrome cases could be fruitful.

370 RMI2 is the fourth component of the BTRR complex. A single family was recently
371 reported with a homozygous deletion of *RMI2* in which two children were also found to
372 have elevated SCEs, with café-au lait macules evident, but mild-growth impairment evident
373 in only one individual[39]. As RMI2 is not essential for BTR (BLM, TopIIIα and RMI1) enzymatic
374 function[13], a more subtle cellular and developmental phenotype might therefore result. It
375 also remains possible that the BTR complex has functions independent of RMI2, given that
376 BLM, TopIIIα and RMI1 are conserved in all eukaryotes but RMI2 is absent in invertebrates
377 and yeast [14].

378 Bloom's syndrome is associated with predisposition to both solid tumors and
379 haematological malignancies[3]. However, cancers have not been reported in our cases with
380 *TOP3A* mutations. Nevertheless, all are still children and as malignancy in Bloom's typically
381 manifests in early adulthood, *TOP3A* mutations may well also confer increased risk of
382 neoplasia.

383 Distinct from Bloom's syndrome, some of our *TOP3A* subjects have clinical features
384 consistent with mitochondrial dysfunction, with several exhibiting a dilated

cardiomyopathy. Notably, an individual with chronic progressive external ophthalmoplegia and cerebellar ataxia has been recently reported, along with a novel functional role for TopIIIα in the decatenation of mitochondrial DNA following its replication[34] (in this manuscript denoted as subject, MC1). The compound heterozygous mutations c.298A>G; c. 403C>T; p. Met100Val; pArg135* may have milder consequences than those reported in our cohort, and consistent with this we found that MC1 does not exhibit short stature (Table 2) or elevated numbers of SCEs in a primary fibroblast line derived from this individual (Figure S2). Thus, it appears that the residual TopIIIα activity in MC1 is sufficient for the nuclear function of the BTRR complex in dHJ dissolution and for normal growth, but may have become rate-limiting for the role of TopIIIα in mitochondrial DNA replication.

Mechanistically, our cellular and biochemical studies suggest that the identified *TOP3A* mutations reported here are severe hypomorphs, consistent with the established essential cellular and developmental functions of TopIIIα[35]. Given that marked growth restriction is common to *TOP3A* and *BLM* subjects, it seems likely that they have a shared pathogenic basis arising from reduced ssDNA decatenation activity of the BTRR complex. Persistence of unresolved hemicatenanes into mitosis leads to formation of chromatin and ultra-fine mitotic bridges that have previously been reported in Bloom's syndrome [20] and in microcephalic dwarfism individuals with condensin mutations[40]. The resulting genome instability arising from persistent chromatin bridges [41; 42] and micronuclei[43] may therefore impair cell viability during development, causing microcephaly and global growth restriction. In summary, we demonstrate that mutations in *TOP3A* cause microcephalic dwarfism with increased SCE, implicating the BTRR complex as a cause of growth disorders.

Supplemental Data description

Three supplementary figures and a table are provided.

Acknowledgements

We thank the families and clinicians for their involvement and participation; the Potentials Foundation and Walking with Giants Foundation; IGMM core sequencing service. G. Stewart, D.Fitzpatrick for helpful discussions. This work was supported by funding from ERC Starter Grant 281847, the Medical Research Council (MRC) Human Genetics Unit core grant U127580972;.the Danish National Research Foundation (DNRF115), the European Research Council (to IDH); Danish Cancer Society postdoctoral fellowship (to RST); MINECO SAF2015-66831-R and SAF2017-84646-R (to KEH); ICREA-Academia program, the Spanish Ministry of Economy and Competiveness project SAF2015-64152-R, the European Commission, the "Fondo Europeo de Desarrollo Regional, una manera de hacer Europa" FEDER, CIBERER an initiative of the Instituto de Salud Carlos III, Spain (to JS); Wellcome Centre for Mitochondrial Research 203105/Z/16/Z, MRC grants G0601943, G0800674, UK NHS Highly Specialised Service for Rare Mitochondrial Disorders of Adults and Children (to RWT, GSG); German Federal Ministry of Education BMBF grant 01GM1404, E-RARE network EuroMicro, German Research Foundation SFB1002 project D02 (to B.W); Practical Research Project for Rare/Intractable Diseases（18ek0109273, 18ek0109177）from Japan Agency for Medical Research and Development, AMED (to K.M, A.O, and Y.O); Great Ormond Street Hospital Children's Charity and NIHR Great Ormond Street Hospital Biomedical Research Centre (to MTD). The views expressed are those of the author(s) and not necessarily those of the NHS, the NIHR or the Department of Health.; National Center for Advancing Translational Sciences, National Institutes of Health, through Grant Number UL1TR001873 (to ARP/AI).

The content is solely the responsibility of the authors and does not necessarily represent the official views of the NIH.

Declaration of Interests

MC and AB are employees of GeneDx, Inc., a wholly owned subsidiary of OPKO Health, Inc. The authors declare no other conflicts of interest.

Web Resources

GnomAD. http://gnomad.broadinstitute.org

Online Mendelian Inheritance in Man. http://www.omim.org

References

1. Klingseisen, A., and Jackson, A.P. (2011). Mechanisms and pathways of growth failure in primordial dwarfism. Genes Dev 25, 2011-2024.
2. Bloom, D. (1954). Congenital telangiectatic erythema resembling lupus erythematosus in dwarfs; probably a syndrome entity. AMA Am J Dis Child 88, 754-758.
3. German, J. (1997). Bloom's syndrome. XX. The first 100 cancers. Cancer Genet Cytogenet 93, 100-106.
4. Chaganti, R.S., Schonberg, S., and German, J. (1974). A manyfold increase in sister chromatid exchanges in Bloom's syndrome lymphocytes. Proc Natl Acad Sci U S A 71, 4508-4512.
5. Sanz, M.M., German, J., and Cunniff, C. (1993). Bloom's Syndrome. In GeneReviews((R)), M.P. Adam, H.H. Ardinger, R.A. Pagon, S.E. Wallace, L.J.H. Bean, K. Stephens, andA. Amemiya, eds. (Seattle (WA).
6. Ellis, N.A., Groden, J., Ye, T.Z., Straughen, J., Lennon, D.J., Ciocci, S., Proytcheva, M., and German, J. (1995). The Bloom's syndrome gene product is homologous to RecQ helicases. Cell 83, 655-666.
7. German, J., Sanz, M.M., Ciocci, S., Ye, T.Z., and Ellis, N.A. (2007). Syndrome-causing mutations of the BLM gene in persons in the Bloom's Syndrome Registry. Hum Mutat 28, 743-753.
8. Johnson, F.B., Lombard, D.B., Neff, N.F., Mastrangelo, M.A., Dewolf, W., Ellis, N.A., Marciniak, R.A., Yin, Y., Jaenisch, R., and Guarente, L. (2000). Association of the Bloom syndrome protein with topoisomerase IIIalpha in somatic and meiotic cells. Cancer Res 60, 1162-1167.
9. Wu, L., Davies, S.L., North, P.S., Goulaouic, H., Riou, J.F., Turley, H., Gatter, K.C., and Hickson, I.D. (2000). The Bloom's syndrome gene product interacts with topoisomerase III. J Biol Chem 275, 9636-9644.
10. Raynard, S., Bussen, W., and Sung, P. (2006). A double Holliday junction dissolvasome comprising BLM, topoisomerase IIIalpha, and BLAP75. J Biol Chem 281, 13861-13864.
11. Wu, L., Bachrati, C.Z., Ou, J., Xu, C., Yin, J., Chang, M., Wang, W., Li, L., Brown, G.W., and Hickson, I.D. (2006). BLAP75/RMI1 promotes the BLM-dependent dissolution of homologous recombination intermediates. Proc Natl Acad Sci U S A 103, 4068-4073.
12. Yin, J., Sobeck, A., Xu, C., Meetei, A.R., Hoatlin, M., Li, L., and Wang, W. (2005). BLAP75, an essential component of Bloom's syndrome protein complexes that maintain genome integrity. EMBO J 24, 1465-1476.
13. Singh, T.R., Ali, A.M., Busygina, V., Raynard, S., Fan, Q., Du, C.H., Andreassen, P.R., Sung, P., and Meetei, A.R. (2008). BLAP18/RMI2, a novel OB-fold-containing protein, is an essential component of the Bloom helicase-double Holliday junction dissolvasome. Genes Dev 22, 2856-2868.
14. Xu, D., Guo, R., Sobeck, A., Bachrati, C.Z., Yang, J., Enomoto, T., Brown, G.W., Hoatlin, M.E., Hickson, I.D., and Wang, W. (2008). RMI, a new OB-fold complex essential for Bloom syndrome protein to maintain genome stability. Genes Dev 22, 2843-2855.
15. Wu, L., and Hickson, I.D. (2003). The Bloom's syndrome helicase suppresses crossing over during homologous recombination. Nature 426, 870-874.
16. Plank, J.L., Wu, J., and Hsieh, T.S. (2006). Topoisomerase IIIalpha and Bloom's helicase can resolve a mobile double Holliday junction substrate through convergent branch migration. Proc Natl Acad Sci U S A 103, 11118-11123.
17. Wechsler, T., Newman, S., and West, S.C. (2011). Aberrant chromosome morphology in human cells defective for Holliday junction resolution. Nature 471, 642-646.
18. Ajima, J., Umezu, K., and Maki, H. (2002). Elevated incidence of loss of heterozygosity (LOH) in an sgs1 mutant of Saccharomyces cerevisiae: roles of yeast RecQ helicase in suppression of aneuploidy, interchromosomal rearrangement, and the simultaneous incidence of both events during mitotic growth. Mutat Res 504, 157-172.

19. Luo, G., Santoro, I.M., McDaniel, L.D., Nishijima, I., Mills, M., Youssoufian, H., Vogel, H., Schultz, R.A., and Bradley, A. (2000). Cancer predisposition caused by elevated mitotic recombination in Bloom mice. Nat Genet 26, 424-429.
20. Chan, K.L., North, P.S., and Hickson, I.D. (2007). BLM is required for faithful chromosome segregation and its localization defines a class of ultrafine anaphase bridges. EMBO J 26, 3397-3409.
21. Cole, T.J., Freeman, J.V., and Preece, M.A. (1998). British 1990 growth reference centiles for weight, height, body mass index and head circumference fitted by maximum penalized likelihood. Stat Med 17, 407-429.
22. Keller, C., Keller, K.R., Shew, S.B., and Plon, S.E. (1999). Growth deficiency and malnutrition in Bloom syndrome. J Pediatr 134, 472-479.
23. Murray, J.E., Bicknell, L.S., Yigit, G., Duker, A.L., van Kogelenberg, M., Haghayegh, S., Wieczorek, D., Kayserili, H., Albert, M.H., Wise, C.A., et al. (2014). Extreme growth failure is a common presentation of ligase IV deficiency. Hum Mutat 35, 76-85.
24. Tanaka, A.J., Cho, M.T., Millan, F., Juusola, J., Retterer, K., Joshi, C., Niyazov, D., Garnica, A., Gratz, E., Deardorff, M., et al. (2015). Mutations in SPATA5 Are Associated with Microcephaly, Intellectual Disability, Seizures, and Hearing Loss. Am J Hum Genet 97, 457-464.
25. Goulaouic, H., Roulon, T., Flamand, O., Grondard, L., Lavelle, F., and Riou, J.F. (1999). Purification and characterization of human DNA topoisomerase IIIalpha. Nucleic Acids Res 27, 2443-2450.
26. Karow, J.K., Chakraverty, R.K., and Hickson, I.D. (1997). The Bloom's syndrome gene product is a 3'-5' DNA helicase. J Biol Chem 272, 30611-30614.
27. Henricksen, L.A., Umbricht, C.B., and Wold, M.S. (1994). Recombinant replication protein A: expression, complex formation, and functional characterization. J Biol Chem 269, 11121-11132.
28. (2001). Human Cytogenetics: malignancy and acquired abnormalities. A Practical Approach (3rd edition).
29. Bizard, A.H., Nielsen, C.F., and Hickson, I.D. (2017). Detection of Ultrafine Anaphase Bridges. Methods Mol Biol 1672, 495-508.
30. Bhowmick, R., Minocherhomji, S., and Hickson, I.D. (2016). RAD52 Facilitates Mitotic DNA Synthesis Following Replication Stress. Mol Cell 64, 1117-1126.
31. Nielsen, C.F., Huttner, D., Bizard, A.H., Hirano, S., Li, T.N., Palmai-Pallag, T., Bjerregaard, V.A., Liu, Y., Nigg, E.A., Wang, L.H., et al. (2015). PICH promotes sister chromatid disjunction and co-operates with topoisomerase II in mitosis. Nat Commun 6, 8962.
32. Sobreira, N., Schiettecatte, F., Valle, D., and Hamosh, A. (2015). GeneMatcher: a matching tool for connecting investigators with an interest in the same gene. Hum Mutat 36, 928-930.
33. Lek, M., Karczewski, K.J., Minikel, E.V., Samocha, K.E., Banks, E., Fennell, T., O'Donnell-Luria, A.H., Ware, J.S., Hill, A.J., Cummings, B.B., et al. (2016). Analysis of protein-coding genetic variation in 60,706 humans. Nature 536, 285-291.
34. Nicholls, T.J., Nadalutti, C.A., Motori, E., Sommerville, E.W., Gorman, G.S., Basu, S., Hoberg, E., Turnbull, D.M., Chinnery, P.F., Larsson, N.G., et al. (2018). Topoisomerase 3alpha Is Required for Decatenation and Segregation of Human mtDNA. Mol Cell 69, 9-23 e26.
35. Li, W., and Wang, J.C. (1998). Mammalian DNA topoisomerase IIIalpha is essential in early embryogenesis. Proc Natl Acad Sci U S A 95, 1010-1013.
36. Hoffelder, D.R., Luo, L., Burke, N.A., Watkins, S.C., Gollin, S.M., and Saunders, W.S. (2004). Resolution of anaphase bridges in cancer cells. Chromosoma 112, 389-397.
37. Lukas, C., Savic, V., Bekker-Jensen, S., Doil, C., Neumann, B., Pedersen, R.S., Grofte, M., Chan, K.L., Hickson, I.D., Bartek, J., et al. (2011). 53BP1 nuclear bodies form around DNA lesions generated by mitotic transmission of chromosomes under replication stress. Nat Cell Biol 13, 243-253.
38. Bocquet, N., Bizard, A.H., Abdulrahman, W., Larsen, N.B., Faty, M., Cavadini, S., Bunker, R.D., Kowalczykowski, S.C., Cejka, P., Hickson, I.D., et al. (2014). Structural and mechanistic insight

into Holliday-junction dissolution by topoisomerase IIIalpha and RMI1. Nat Struct Mol Biol 21, 261-268.
39. Hudson, D.F., Amor, D.J., Boys, A., Butler, K., Williams, L., Zhang, T., and Kalitsis, P. (2016). Loss of RMI2 Increases Genome Instability and Causes a Bloom-Like Syndrome. PLoS Genet 12, e1006483.
40. Martin, C.A., Murray, J.E., Carroll, P., Leitch, A., Mackenzie, K.J., Halachev, M., Fetit, A.E., Keith, C., Bicknell, L.S., Fluteau, A., et al. (2016). Mutations in genes encoding condensin complex proteins cause microcephaly through decatenation failure at mitosis. Genes Dev 30, 2158-2172.
41. Janssen, A., van der Burg, M., Szuhai, K., Kops, G.J., and Medema, R.H. (2011). Chromosome segregation errors as a cause of DNA damage and structural chromosome aberrations. Science 333, 1895-1898.
42. Maciejowski, J., Li, Y., Bosco, N., Campbell, P.J., and de Lange, T. (2015). Chromothripsis and Kataegis Induced by Telomere Crisis. Cell 163, 1641-1654.
43. Crasta, K., Ganem, N.J., Dagher, R., Lantermann, A.B., Ivanova, E.V., Pan, Y., Nezi, L., Protopopov, A., Chowdhury, D., and Pellman, D. (2012). DNA breaks and chromosome pulverization from errors in mitosis. Nature 482, 53-58.

Figure 1. Variants in *TOP3A* are associated with prenatal-onset growth retardation and microcephaly

a) Morphometric data for *TOP3A* individuals. A global reduction in growth is evident from before birth. Z-scores (standard deviations from population mean for age and sex) for birth weight (Wgt), and postnatal weight, height (Hgt) and occipital-frontal circumference (OFC). Dashed lines indicate the 95% confidence interval for the general population. Black circles, TOP3A individual data points. For comparison grey bars indicate the mean value for a cohort of n=89 (birth weight). n=47 (current weight), n=52 (current height) Bloom's syndrome subjects[22].

b) Photographs of facial features of individuals with *TOP3A* mutations.

Figure 2. Mutations in *TOP3A* markedly reduce levels of the TopIIIα protein but do not affect its intrinsic decatenation activity

A) Schematic of TopIIIα protein with locations of variants annotated. Red, TOPRIM domain; purple TOPA domain; blue, GRF zinc finger domain.

B) *TOP3A* mutations markedly reduce protein levels. Immunoblotting of total cell lysates from affected individual derived dermal fibroblast lines as indicated. siRNA depletion of TOP3A in control 2 fibroblast line to confirm specificity of antibody. C1 and C2 unrelated control fibroblast lines. (TopIIIα antibody raised against amino acids 652-1001).

C) Recombinant TopIIIα^{Thr812LeufsTer101} protein (denoted TopIIIα^{P1}) is less stable than TopIIIα^{WT}. Immunoblot of purified TopIIIα^{WT} and TopIIIα^{P1} probed with TopIIIα antibody. Protein size markers 250, 170, 140, 100, 70 kDa

D) Schematic depicting the BTRR complex and its role in double Holliday junction (dHJ) dissolution. Homologous sister chromatids are shown in red and blue respectively.

E-F) TopIIIα^{P1} protein is proficient for promoting dHJ dissolution with BLM in combination with the RMI1 and RMI2 proteins. E) Representative polyacrylamide gel demonstrating the enzyme concentration dependence of the dHJ dissolution activity of TopIIIα^{WT} and mutant (TopIIIα^{P1}) TRR complexes with 20 nM BLM at 37°C in 30 min. TRR was included in reactions at increasing concentrations ranging from 20 pM-10

nM. Labelled circular oligonucleotide (lane 1) and dHJ (lane 2) were included as markers. F) Quantification of the dHJ dissolution reaction shown in panel E. The reaction was repeated two more times with very similar results.

Figure 3. *TOP3A* individuals have elevated levels of SCEs reflecting chromatid hyper-recombination

A) Schematic of dHJ processing . dHJ are either dissolved by the BTRR complex or alternatively cleaved by structure specific nucleases that lead to dHJ resolution.

B-C) Elevated numbers of SCEs are evident from BrdU strand specific labelling of sister chromatids from TOP3A cells compared to control and parent cells. B) Representative images of P1 and parent fibroblast cell lines. C) Quantification of SCEs in fibroblast cell lines (P1, P5, P7, P8) or PHA-stimulated lymphocytes derived from peripheral blood samples (P2, P3). Median value plotted, n>10 metaphase spreads counted per subject. Pair-wise non-parametric Mann Whitney tests versus parental controls. F1, F2 and F5 SCEs were scored in independent laboratories.

Figure 4. DNA catenanes persist into mitosis in *TOP3A* subject cells leading to chromosome segregation defects and genome instability

A-B) Chromosome segregation is impaired in *TOP3A* deficient primary fibroblasts. A) Representative images of chromatin bridges, lagging DNA (DAPI) and ultrafine DNA bridges (UFBs) (detected by the presence of PICH and absence of DAPI stain). B) Quantification of chromatin bridges, lagging DNA and PICH positive UFBs scored in Control, parental and P1 fibroblast mitotic cells staged at anaphase B (exp≥3, n> 50 cells, error bars = SEM). To enrich for mitotic cells, fibroblasts were treated with R03306 for 6 hrs, released and fixed after 45 min. C) *TOP3A* P1 fibroblast cells display significantly elevated levels of micronuclei. Top panel, representative picture of control and P1 fibroblasts. Bottom panel, Quantification of micronucleus containing interphase cells. exp≥3, n>500, error bars = SEM. To enrich for G1 cells, RO3306 treated cells were released into fresh media for 30 mins, prometaphase cells were collected, re-seeded and fixed after 4-6 hrs. D) *TOP3A* P1 fibroblast cells display significantly elevated numbers of 53BP1 bodies in G1 nuclei. Top panel, representative images of 53BP1 foci (red) and DNA (DAPI). Bottom panel, quantification of cells with ≥4 53BP1 foci in G1 nuclei (negative for cyclin A) (exp≥3, n>500, error bars = SEM). Scale bar = 2 microns, Two tailed t-test versus parent.

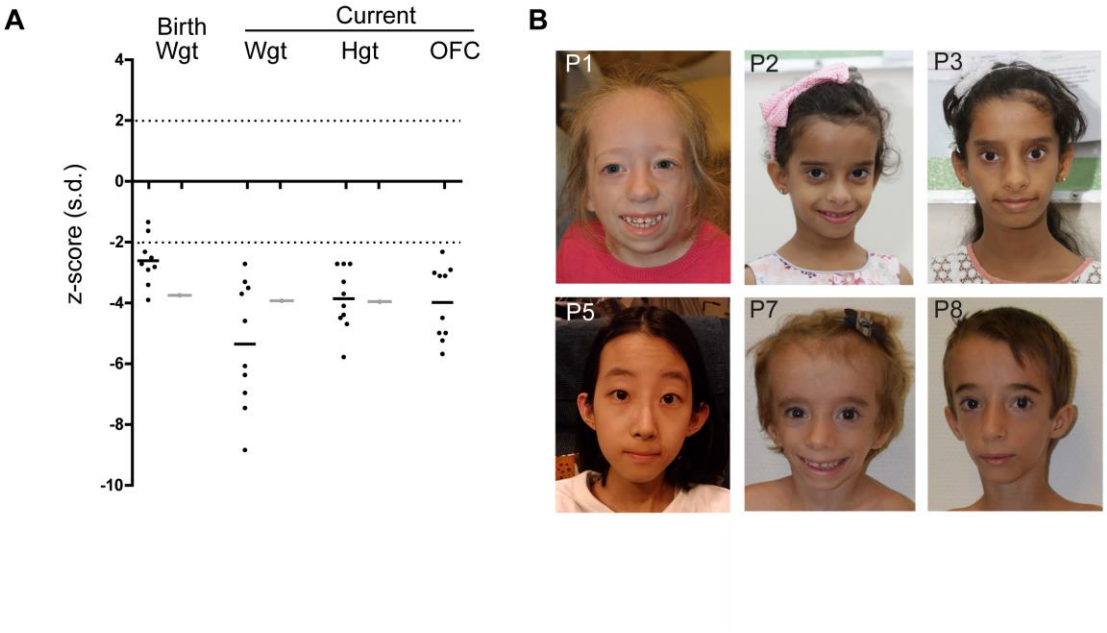
A
Birth
Wgt
Current
Wgt
Hgt
OFC
z-score (s.d.)
4
2
0
-2
-4
-6
-8
-10
B
P1
P2
P3
P5
P7
P8

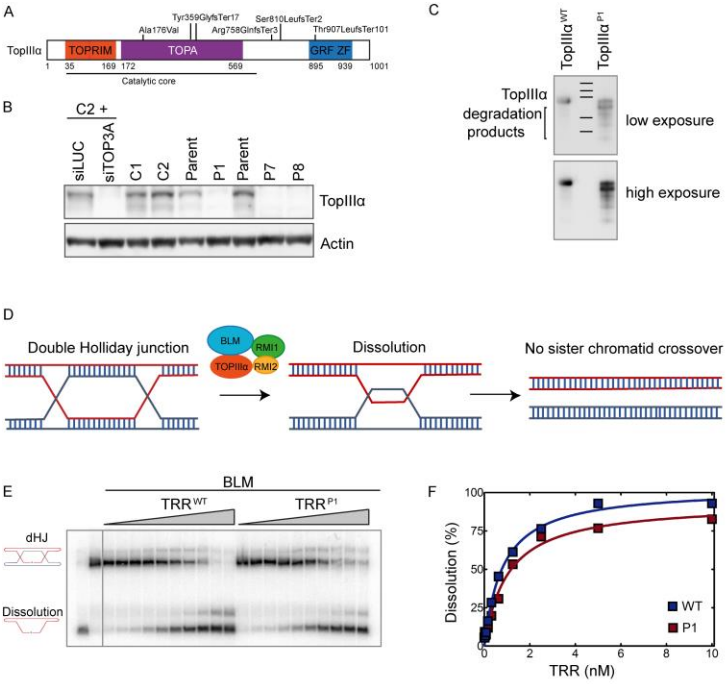
A
Tyr359GlyfsTer17
Ala176Val
Arg758GlnfsTer3
Ser810LeufsTer2
Thr907LeufsTer101
TopIIIα
TOPRIM
TOPA
GRF ZF
1
35
169
172
569
895
939
1001
Catalytic core
B
C2 +
siLUC
siTOP3A
C1
C2
Parent
P1
Parent
P7
P8
TopIIIα
Actin
C
TopIIIα WT
TopIIIα P1
TopIIIα degradation products
low exposure
high exposure
D
Double Holliday junction
BLM
RMI1
TOPIIIα
RMI2
Dissolution
No sister chromatid crossover
E
BLM
TRR WT
TRR P1
dHJ
Dissolution
F
Dissolution (%)
100
75
50
25
0
2
4
6
8
10
TRR (nM)
WT
P1

613

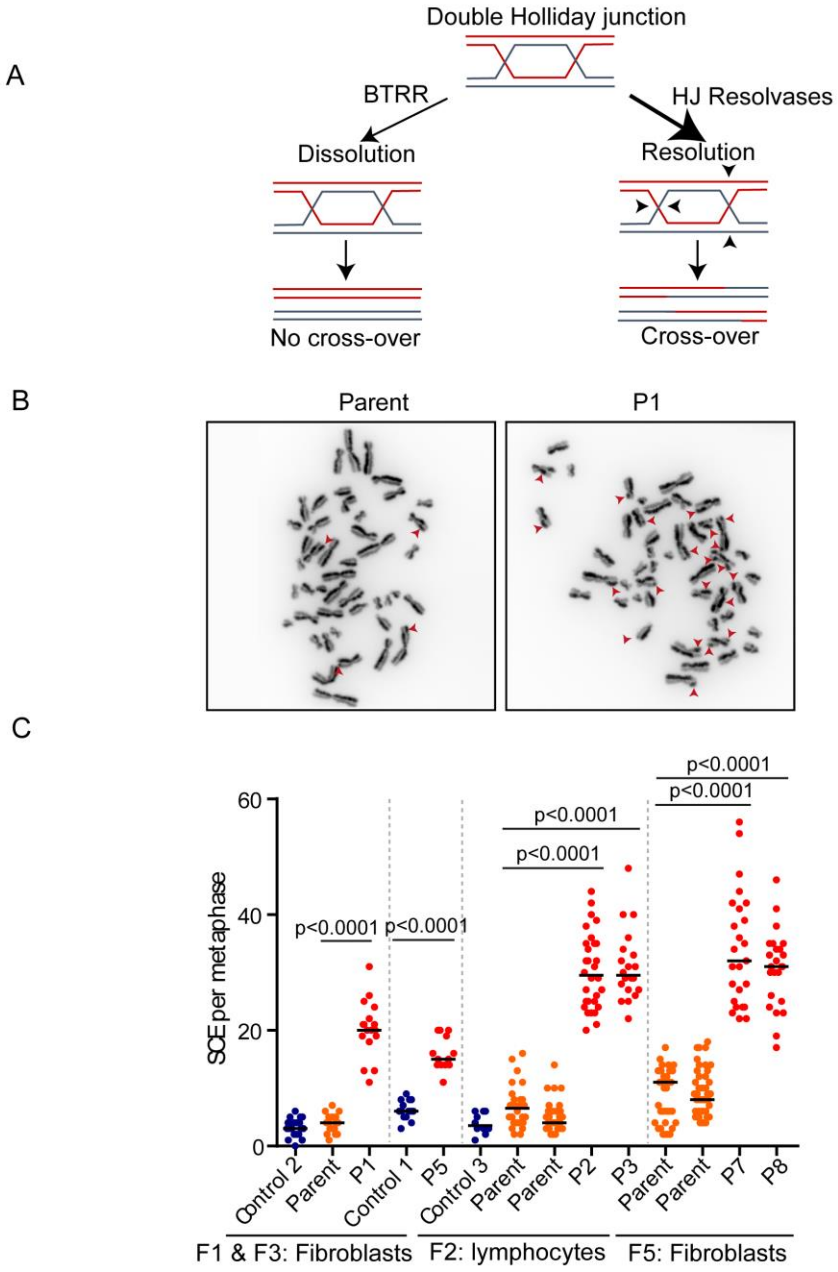
A
Double Holliday junction
BTRR
HJ Resolvases
Dissolution
Resolution
No cross-over
Cross-over
B
Parent
P1
C
SCE per metaphase
60
40
20
0
p<0.0001
p<0.0001
p<0.0001
p<0.0001
p<0.0001
Control 2
Parent
P1
Control 1
P5
Control 3
Parent
Parent
P2
P3
Parent
Parent
P7
P8
F1 & F3: Fibroblasts
F2: lymphocytes
F5: Fibroblasts

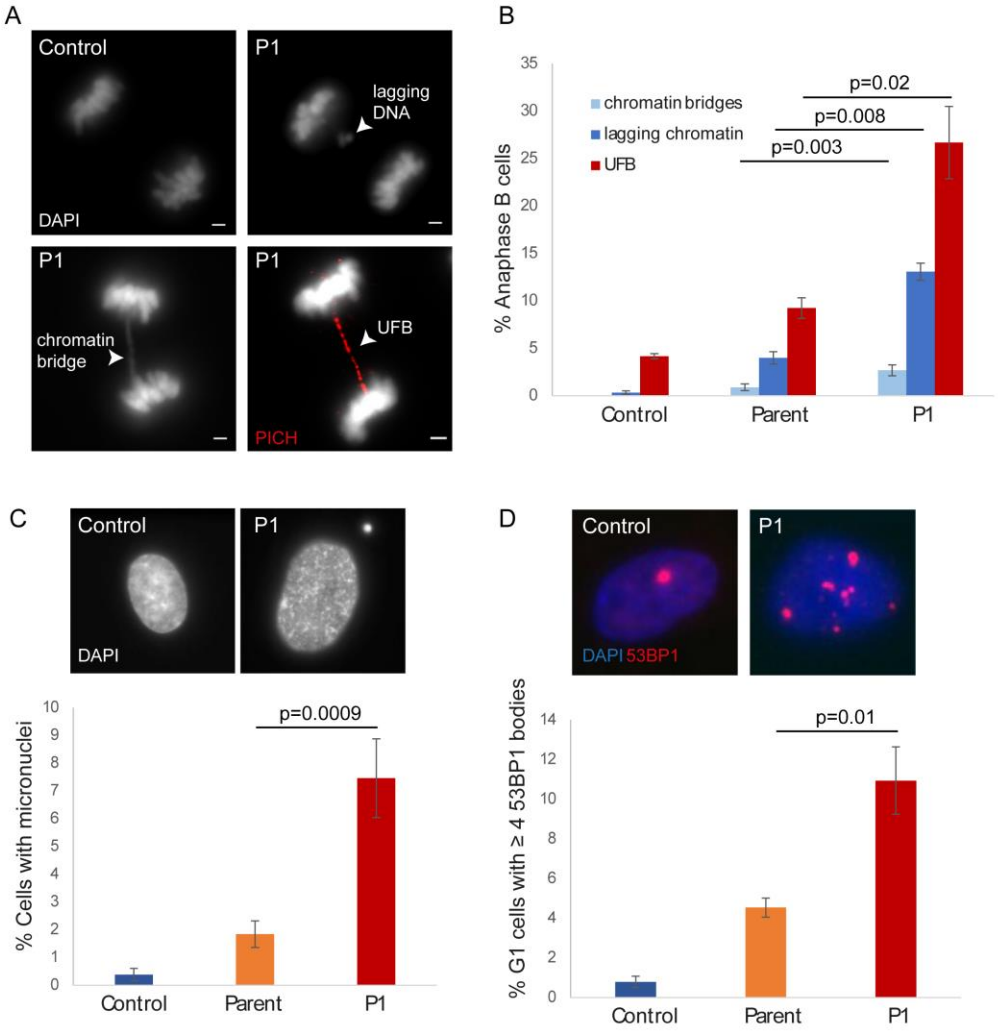
A
Control
DAPI
P1
lagging DNA
P1
chromatin bridge
P1
UFB
PICH
B
% Anaphase B cells
chromatin bridges
lagging chromatin
UFB
p=0.02
p=0.008
p=0.003
Control
Parent
P1
C
Control
DAPI
P1
% Cells with micronuclei
p=0.0009
Control
Parent
P1
D
Control
DAPI 53BP1
P1
% G1 cells with ≥ 4 53BP1 bodies
p=0.01
Control
Parent
P1

615

Table 1. Variants Identified in *TOP3A* and *RMI1* associated with microcephalic dwarfism

Family	Individual	Gene	Biallelic Nucleotide Alterations	Predicted Amino Acid Consequence(s)	Sex	Country of origin
1	P1	*TOP3A*	c.[2718del];[2718del]	p.[Thr907LeufsTer101];[Thr907LeufsTer101]	Female	USA (Czech/Irish ancestry)
2	P2	*TOP3A*	c.[2271dup];[2271dup]	p.[Arg758GlnfsTer3];[Arg758GlnfsTer3]	Female	United Arab Emirates
2	P3	*TOP3A*	c.[2271dup];[2271dup]	p.[Arg758GlnfsTer3];[Arg758GlnfsTer3]	Female	United Arab Emirates
2	P4	*TOP3A*	c.[2271dup];[2271dup]	p.[Arg758GlnfsTer3];[Arg758GlnfsTer3]	Male	United Arab Emirates
3	P5	*TOP3A*	c.[527C>T];[1072_1073dup][a]	p.[Ala176Val];[Tyr359GlyfsTer17]	Female	Japan
4	P6	*TOP3A*	c.[2271dup];[2271dup]	p.[Arg758GlnfsTer3];[Arg758GlnfsTer3]	Female	Syria
5	P7	*TOP3A*	c.[2428del];[2428del]	p.[Ser810LeufsTer2];[Ser810LeufsTer2]	Female	Spain
5	P8	*TOP3A*	c.[2428del];[2428del]	p.[Ser810LeufsTer2];[Ser810LeufsTer2]	Male	Spain
6	P9	*TOP3A*	c.[2771dup]; c.[2771dup]	p. [Arg758GlnfsTer3];[Arg758GlnfsTer3]	Male	Syria
7	P10	*TOP3A*	c.[2771dup]; c.[2771dup]	p. [Arg758GlnfsTer3];[Arg758GlnfsTer3]	Female	Saudi Arabia
8	P11	*RMI1*	c.[1255_1259del];[1255_1259del]	p.[Lys419LeufsTer5]; [Lys419LeufsTer5]	Female	Turkey
8	P12	*RMI1*	c.[1255_1259del];[1255_1259del]	p.[Lys419LeufsTer5] ;[Lys419LeufsTer5]	Female	Turkey
Previously reported case with adult-onset mitochondrial disease						
	MC1[b]	*TOP3A*	*c.[298A>G];[403C>T]*	*p.[Met100Val];[Arg135Ter]*	*Female*	*UK*

[a] close to donor splice site of exon 10. [b] previously reported case in [34]. Nomenclature according to transcript NM_004618.4, TOP3A; NM_004618.4 and NM_024945.2, RMI1.

Table 2. Growth parameters of *TOP3A* and *RMI1* individuals.

	Birth								Postnatal						
Pt	Gene mutated	Gest[n] (weeks)	Weight kg	SD[a]	OFC cm	SD	Length cm	SD	Age at Exam	Weight kg	SD[a]	OFC cm	SD	Height cm	SD
P1	*TOP3A*	37	1.35	-3.9	27.5	-4.2	38	-5.4	5m	4.9	-2.7	36	-5.7	54.8	-4.4
P2	*TOP3A*	37	1.9	-2.3	N/A	N/A	N/A	N/A	3y	9.5	-3.7	47.5	-2.3	84.5	-2.8
P3	*TOP3A*	37	2.2	-1.6	N/A	N/A	N/A	N/A	8 y	16.5	-3.3	49.5	-2.9	112.5	-2.7
P4	*TOP3A*	40	2.2	-2.9	N/A	N/A	N/A	N/A	10 y	18.1	-4.6	49.5	-3.1	113	-4.1
P5	*TOP3A*	35	1.91	-1.3	31.8	-0.2	43	-1.8	15 y	20	-6.4	51	-3.1	138	-3.7
P6	*TOP3A*	N/A	2	N/A	N/A	N/A	N/A	N/A	19 m	5.17	-7.5	44.3	-3.0	64.3	-5.8
P7	*TOP3A*	38	1.90	-2.8	30.0	-2.7	41	-4.1	3 y 3m	7.21	-7.0	44.2	-5.3	78.7	-4.7
P8	*TOP3A*	34	1.41	-2.5	28.5	-2.2	42	-2.1	7 y[b]	10	-2.9	45.8	-5.0	98.1	-4.5
P9	*TOP3A*	40	2	-3.4	N/A	N/A	N/A	N/A	11 y	21.6	-3.5	47.5	-4.5	125.6	-2.7
P10	*TOP3A*	36	1.6	-2.7	N/A	N/A	N/A	N/A	4 y 7 m	9	-6.1	45.5	-5.0	91	-3.3
P11	*RMI1*	34	1.59	-1.7	N/A	N/A	N/A	N/A	7 y	14	-3.8	46.5	-5	100	-4
P12	*RMI1*	38	1.80	-3.1	N/A	N/A	N/A	N/A	13 y	39	-0.9	48	-5	135	-2.9
Previously reported case with Adult onset-mitochondrial disease (ataxia, PEO)															
MC1	*TOP3A*	N/A	N/A	N/A	N/A	N/A	N/A	N/A	adult	N/A	N/A	N/A	N/A	163	N/A

Gest[n], Gestational age. [a]Adjusted for gestation; [b] on growth hormone treatment 4 years 3 months until 5years 11 months with no response. Z-score, standard deviations from population mean for age and sex. y, year; m, months.

	TOP3A											*RMI1*	
Pt	**P1**	**P2**	**P3**	**P4**	**P5**	**P6**	**P7**	**P8**	**P9**	**P10**	**MC1[R1]**	**P11**	**P12**
Age	5 m	3 y	8 y	10y	15 y	19 m	3 y	7 y	11y	4y 7m	Adult	7 y	13 y
Prenatal onset growth restriction	Y	Y	Y	Y	Y	Y	Y	Y	Y	Y	N	Y	Y
Elevated Sister chromatid exchange	Y	Y	Y	N/A	Y	N/A	Y	Y	Y	N/A	N	N/A	N/A
Café-au-lait macules	Y	Y	Y	Y	N	Y	N	Y	Y	Y	N/A	N	N
Developmental Delay	Mild	N	N	N	N	Mild[e]	N	Mild	N	Mild	N/A	Mild	N
Cancer[a]	N	N	N	N	N	N	N	N	N	N	N/A	N	N
Decreased subcutaneous fat	N	N	N	N	N	N	Y	Y	N	Y	N/A	N	N
Gastrooesophageal reflux	Y	N/A	N/A	N/A	N	Y	N	N/A	N	N/A	N/A	N	N
Diabetes mellitus	N	N	N	N	N	N	N	N	N	N	N/A	N	N
Recurrent infections	Y[b]	N/A	N/A	N/A	N	N	N		Y	Y[h]	N/A	N	N
Malar Rash	N	N	N	N	N	N	N	N	N	N	N/A	N	N
Dilated Cardiomyopathy	N	N	Y	Y (severe, deceased)	Y (post heart transplant)	Normal Echo	N/A	Y[c] (asymptomatic)	HCM[f]	N		N/A	N/A
Mitochondrial DNA depletion in muscle	N/A	N/A	N/A	N/A	Y, 87%	N/A	N/A	N/A	N/A	N/A	Y, >80%	N/A	N/A
Other	CDH, Gastrostomy		Abnormal movements/tics		Hearing loss, CMMA[d]				Microcytic anemia[g]		PEO, Ataxia		

Table 3. Clinical phenotype of *TOP3A* and *RMI1* subjects.

[a]Note all cases <15y old, in Bloom's syndrome, neoplasia typically early adulthood. PEO, progressive external ophthalmoplegia. CDH, Congenital dislocation of hip. [b]Recurrent otitis media and tonsillitis – tonsillectomy. [c]Mild left ventricle dilatation. [d]Combined malonic and methylmalonic aciduria (OMIM#614265) due to *ACSF3* mutations. [e] Expressive speech delay only. [f]HCM, hypertrophic cardiomyopathy. [g]Anemia due to beta-thalassemia trait. [h]Reccurent upper respiratory tract infections/oral thrush.